

1 **Methyl ketone production by *Pseudomonas putida* is enhanced by plant-**  
2 **derived amino acids**

3 Jie Dong<sup>1,2</sup>, Yan Chen<sup>1,2</sup>, Veronica Teixeira Benites<sup>1,2</sup>, Edward E.K. Baidoo<sup>1,2</sup>, Christopher J.  
4 Petzold<sup>1,2</sup>, Harry R. Beller<sup>1,3</sup>, Aymerick Eudes<sup>1,4</sup>, Henrik V. Scheller<sup>1,4</sup>, Paul D. Adams<sup>1,5</sup>,  
5 Aindrila Mukhopadhyay<sup>1,2,4</sup>, Blake A. Simmons<sup>1,2</sup>, Steven W. Singer<sup>1,2\*</sup>

6  
7 <sup>1</sup>Joint BioEnergy Institute, Emeryville, CA, 94608; <sup>2</sup>Biological Systems and Engineering  
8 Division, Lawrence Berkeley National Laboratory, Berkeley, CA, 94720; <sup>3</sup>Earth and  
9 Environmental Sciences Area, Lawrence Berkeley National Laboratory, Berkeley, CA, 94720;  
10 <sup>4</sup>Environmental Genomics and Systems Biology Division, Lawrence Berkeley National  
11 Laboratory, Berkeley, CA, 94720; <sup>5</sup>Molecular Biophysics and Integrated Bioimaging Division,  
12 Lawrence Berkeley National Laboratory, Berkeley, CA, 94720

13

14 \*Corresponding author:  
15 Joint BioEnergy Institute  
16 5885 Hollis Street  
17 Emeryville, CA 94608  
18 Phone: (510) 495-2492  
19 Fax: (510) 486-4252  
20 E-mail: [SWSinger@lbl.gov](mailto:SWSinger@lbl.gov)

21

22

23 **ABSTRACT**

24  
25 Plant biomass is an attractive source of renewable carbon for conversion to biofuels and bio-  
26 based chemicals. Conversion strategies often use a fraction of the total biomass, focusing on  
27 sugars from cellulose and hemicellulose. Strategies that use plant components such as plant-  
28 derived aromatics and amino acids have the potential to improve the efficiency of overall  
29 biomass conversion. *Pseudomonas putida* is a promising host for biomass conversion for its  
30 ability to metabolize a wide variety of organic compounds, including aromatics derived from  
31 lignin. *P. putida* was engineered to produce medium chain methyl ketones, which are promising  
32 diesel blendstocks and potential platform chemicals, from glucose and lignin-related aromatics,  
33 4-hydroxybenzoate (4-HB) and protocatechuate (PCA). Unexpectedly, *P. putida* methyl ketone  
34 production was enhanced 2-to 5-fold compared to sugar controls when *Arabidopsis thaliana*  
35 hydrolysates derived from engineered plants that overproduce 4-HB and PCA, while *E. coli*  
36 production was lowered in these hydrolysates. This enhancement was more pronounced (~7-fold  
37 increase) with hydrolysates derived from non-engineered switchgrass (*Panicum virgatum* L.)  
38 suggesting it did not arise from overproduction of 4-HB and PCA. Global proteomic analysis of  
39 the methyl ketone-producing *P. putida* suggested that plant-derived amino acids may be the  
40 source of this enhancement. Mass spectrometry-based measurements of plant-derived amino  
41 acids demonstrated a high correlation between methyl ketone production and amino acid  
42 concentration in plant hydrolysates. Amendment of glucose-containing minimal media with a  
43 defined mixture of amino acids similar to those found in the hydrolysates studied led to a 9-fold  
44 increase in methyl ketone titer (1.1 g/L).

45 **Keywords: lignin-related aromatics; methyl ketones; biomass hydrolysates; protein; amino**  
46 **acids.**

## 47 INTRODUCTION

48 Plant biomass is an abundant potential resource for the production of biofuels and bio-based  
49 chemicals (Fiorentino, Ripa, & Ulgiati, 2017). The secondary plant cell walls are mainly  
50 composed of polysaccharides (cellulose, hemicellulose) and lignin, a complex polymer  
51 synthesized from aromatic monomers (Pandey & Kim, 2011). Conversion and upgrading of plant  
52 biomass has focused on C6 (cellulose) and C5 (hemicellulose) sugars obtained by  
53 physiochemical pretreatment and enzymatic hydrolysis of the cell-wall polysaccharides. The  
54 residual lignin is often combusted for its heating value; however, multiple methods exist to  
55 depolymerize lignin by chemical and biological processes (Zakzeski, Bruijninx, Jongerius, &  
56 Weckhuysen, 2010)(Bugg, Ahmad, Hardiman, & Singh, 2011). These depolymerized lignins can  
57 be converted by microorganisms that can use these monoaromatic lignin-related compounds as  
58 bioconversion substrates (Beckham, Johnson, Karp, Salvachúa, & Vardon, 2016). Recent work  
59 has taken advantage of the ability of certain soil bacteria, particularly *Pseudomonas putida* and  
60 *Rhodococcus opacus*, to funnel lignin-related monoaromatics towards the production of  
61 polyhydroxyalkanoates, triacylglycerides and *cis*, *cis*-muconic acid (Linger et al.,  
62 2014)(Andreoni, Bernasconi, Bestetti, & Villa, 1991)(Vardon et al., 2015).

63

64 Bioconversion studies with lignin-related aromatics have focused on purified substrates (*p*-  
65 coumarate, 4-hydroxybenzoate, vanillate) or mixtures of aromatics obtained by chemical  
66 depolymerization of lignin. *Arabidopsis thaliana* and tobacco plants have been engineered with  
67 bacterial enzymes that shunt intermediates of lignin biosynthesis to alter lignin structures and  
68 lower plant lignin content (Eudes et al., 2015)(Eudes et al., 2012)(Wu et al., 2017). These  
69 engineered plants display an increase in saccharification efficiency when treated with

70 cellulase/xylanase mixtures. As a byproduct of these transformations, soluble monoaromatics,  
71 which were present in the plant as aromatic glucosides, are produced at 1-5% of the total  
72 biomass. These soluble aromatics were extracted with organic solvent and treated under mild  
73 acidic conditions to release the deglycosylated monoaromatics (Eudes et al., 2015).  
74 Monoaromatics extracted from tobacco plants expressing dehydroshikimate dehydratase (QsuB)  
75 from *Corynebacterium glutamicum* were highly enriched in PCA(~5% of total biomass), and  
76 these extracts were incubated with engineered *Escherichia coli* strains that produced *cis, cis*-  
77 muconic acid (Wu et al., 2017). Therefore, these engineered plants may provide a direct method  
78 to produce lignin-related monoaromatics without requiring energy-intensive thermochemical  
79 treatments of lignin in order to liberate them.

80

81 Products obtained by engineering microbial fatty acid biosynthetic pathways (C<sub>10</sub>-C<sub>18</sub>) are  
82 attractive targets as precursors to biofuels and biochemicals. Free fatty acids, which have been  
83 overproduced in multiple microbes, can be converted to hydrocarbons and fatty acid ethyl esters,  
84 which are useful as diesel replacements or blendstocks (Beller, Lee, & Katz, 2015). Fatty  
85 alcohols, which are derived from free fatty acids by reduction, can be used as surfactants and  
86 lubricants (Espaux et al., 2017). Decarboxylation of beta-keto acids, an intermediate in fatty acid  
87 beta-oxidation, produces methyl ketones, which can also serve as diesel blendstocks as well as  
88 ingredients in the flavor and fragrance industry (Goh, Baidoo, Keasling, & Beller, 2012). Methyl  
89 ketones are particularly attractive as biofuel targets because they freely diffuse from cells and  
90 can be captured in an organic solvent overlay. Unlike free fatty acids, methyl ketones do not  
91 require additional processing steps to be blended into conventional diesel fuels. Methyl ketone  
92 production has been most intensively studied in *E. coli*, for which a titer of 3.4-5.4 g/L was

93 achieved by fed-batch glucose fermentation (Goh et al., 2014)(Goh, Chen, Petzold, Keasling, &  
94 Beller, 2018). Methyl ketone production has also been demonstrated under fed-batch glucose  
95 fermentation in oleaginous yeast *Yarrowia lipolytica* (315 mg/L) (Hanko et al., 2018) and under  
96 autotrophic conditions from H<sub>2</sub>/CO<sub>2</sub> in *Ralstonia eutropha* (180 mg/L) (Müller et al., 2013).

97

98 Here we describe the engineering of *P. putida* to produce medium chain methyl ketones from  
99 both glucose and lignin-related aromatics. Unexpectedly, methyl ketone production experiments  
100 with hydrolysates obtained from engineered *A. thaliana* plants that overproduce monoaromatics  
101 demonstrated significant improvements in methyl ketone production. These improvements were  
102 correlated with amino acid levels in the hydrolysate, rather than the presence of increased levels  
103 of these monoaromatics.

104

105

106

107

108

## 109 MATERIALS AND METHODS

### 110 *Bacterial strains, media, and cultivation.*

111 *Pseudomonas putida* mt-2 (ATCC 33015) and *E. coli* S17-1 (ATCC 47055) were purchased  
112 from ATCC. *E. coli* DH5 $\alpha$  was purchased from Thermo Fisher Scientific. *E. coli* EGS1895 (Goh  
113 et al., 2014) was obtained from the JBEI Registry (Table 1). *E. coli* S17-1 and *E. coli* DH5 $\alpha$  were  
114 propagated at 37 °C in lysogeny broth (LB). Where necessary, medium was solidified with 1.0%  
115 (w/v) agar and supplemented with 50  $\mu$ g/ml kanamycin. *P. putida* mt-2 and its engineered  
116 derivatives were grown at 30 °C in minimal medium (Rocha, da Silva, Taciro, & Pradella, 2008)  
117 (Ouyang, Liu, Fang, & Chen, 2007): (NH<sub>4</sub>)<sub>2</sub>SO<sub>4</sub> 1.0 g/L, KH<sub>2</sub>PO<sub>4</sub> 1.5 g/L, Na<sub>2</sub>HPO<sub>4</sub> 3.54 g/L,  
118 MgSO<sub>4</sub>·7H<sub>2</sub>O 0.2 g/L, CaCl<sub>2</sub>·2H<sub>2</sub>O 0.01 g/L, ammonium ferric citrate 0.06 g/L and trace  
119 elements (H<sub>3</sub>BO<sub>3</sub> 0.3 mg/L, CoCl<sub>2</sub>·6H<sub>2</sub>O 0.2 mg/L, ZnSO<sub>4</sub>·7H<sub>2</sub>O 0.1 mg/L, MnCl<sub>2</sub>·4H<sub>2</sub>O 0.03  
120 mg/L, NaMoO<sub>4</sub>·2H<sub>2</sub>O 0.03 mg/L, NiCl<sub>2</sub>·6H<sub>2</sub>O 0.02 mg/L, CuSO<sub>4</sub>·5H<sub>2</sub>O 0.01 mg/L). Glucose,  
121 xylose, *p*-hydroxybenzoic acid or protocatechuic acid (pH was readjusted to 7.2) or biomass  
122 hydrolysate were supplemented as carbon source. *E. coli* EGS1895 was grown at 37 °C in M9-  
123 MOPS minimal medium (M9 medium supplemented with 75 mM MOPS, 2 mM MgSO<sub>4</sub>, 1 mg/L  
124 thiamine, 10 nM FeSO<sub>4</sub>, 0.1mM CaCl<sub>2</sub>, 56 mM NH<sub>4</sub>Cl and micronutrients including 3 mM  
125 (NH<sub>4</sub>)<sub>6</sub>Mo<sub>7</sub>O<sub>24</sub>, 0.4 mM boric acid, 30 mM CoCl<sub>2</sub>, 15 mM CuSO<sub>4</sub>, 80 mM MnCl<sub>2</sub>, and 10 mM  
126 ZnSO<sub>4</sub>) (Zhang, Carothers, & Keasling, 2012).

127

### 128 *Deletion of P. putida pha operon*

129 The *pha* operon knockout of *P. putida* mt-2 was performed as previously described with some  
130 modifications (Ouyang, Liu, et al., 2007). *P. putida* mt-2 genome DNA was purified by QIAamp  
131 DSP DNA Mini Kit (Qiagen). A fragment from *P. putida* mt-2 genome containing a partial

132 length of *phaC1*, and the whole length of *phaZ* and *phaC2* were amplified by PCR using the  
133 following two primers: 5' primer AGAAAGCTTACCGGCAGCAAGGAC and 3' primer  
134 GAGGCTAGCATCCAGTCAGCAGCTC. PCR products were digested by *NheI* and *HindIII*  
135 and then inserted in pK18mobsacB to form a new plasmid. The new plasmid was amplified in *E.*  
136 *coli* DH5 $\alpha$  and completely digested by *PvuI*, and then the large fragment was self-ligated to form  
137 pJD1. As a result, partial 5' sequence of *phaC1* (0.45 kbp) and partial 3' sequence of *phaC2*  
138 (0.38 kbp) were inserted into pK18mobsacB in pJD1. Then pJD1 was transformed into *E. coli*  
139 S17-1 by electroporation. Transconjugations of *P. putida* mt-2 and *E. coli* S17-1 harboring  
140 recombinant plasmid pJD02 were carried out as previously described (Choi & Schweizer, 2005).  
141 Pseudomonas Isolation Agar (Difco) supplemented with 50  $\mu$ g/mL kanamycin was used to select  
142 transconjugants. Then non-antibiotic LB agar plates supplemented with 250 g/L sucrose were  
143 used to select deletion mutants from transconjugants. The deletion mutants were verified by PCR  
144 using the same primers as those used in plasmid construction.

145

#### 146 *Deletion of P. putida fadAB*

147 The *fadAB* operon deletion in *P. putida* mt-2 was performed as described previously with some  
148 modifications (Ouyang, Luo, et al., 2007). A fragment from the *P. putida* mt-2 genome  
149 containing a partial length of *fadB* and *fadA* were amplified by PCR using the following two  
150 primers: 5' primer ATTTCTAGAGCAGATGATGGCCTTC and 3' primer  
151 CTGAAGCTTTGTAATGCCGGTATAC. PCR products and pK18mobsacB were double-  
152 digested by *XbaI* and *HindIII* and then ligated together to form a new plasmid. The new plasmid  
153 was completely digested by *Sall*, and then the large fragment was self-ligated to form pJD2. As a  
154 result, two DNA fragments, *fadB'* and *fadA'*, corresponding to a partial 5' sequence of *fadB* and

155 partial 3' sequence of *fadA* was inserted into pK18mobsacB in pJD2. The homologous  
156 recombination of pJD04 into *P. putida* mt-2 chromosome and selection of knockout mutants  
157 were carried out as above in the *phaCZC* knockout. Repeating the above *fadAB* knockout  
158 procedure in the *phaCZC* deletion mutants provided a *P. putida* strain with both *fadAB* and  
159 *phaCZC* in-frame deletions.

160

### 161 *Transformation of methyl ketone production pathway into P. putida*

162 The plasmid pJM20 encoding the methyl ketone production pathway was constructed previously  
163 (Müller et al., 2013). It contains the backbone from the broad-host-range vector pBBR1-MCS2  
164 and has *tesA*, *fadB*, *Mlut\_11700*, and *fadM* under the control of BAD promoter (P<sub>BAD</sub>). pJM20  
165 was constructed by inserting a 2-bp deletion in the 3'-end of P<sub>BAD</sub> to prevent inhibition of  
166 arabinose-induction in the presence of glucose (Miyada, Stoltzfus, & Wilcox, 1984). pJM20 was  
167 electroporated into *E.coli* DH5 $\alpha$  for amplification (Johnson & Beckham, 2015) and was  
168 subsequently transferred into *P. putida* mt-2 mutants by electroporation (Johnson & Beckham,  
169 2015). For transformation, 5  $\mu$ L (0.2 -2  $\mu$ g) of plasmid DNA was added to 50  $\mu$ L of the  
170 electrocompetent cells, transferred to a chilled 0.2 cm electroporation cuvette, and  
171 electroporation was performed (1.6 kV, 25 uF, 200  $\Omega$ ). SOC medium (450  $\mu$ L, New England  
172 Biolabs, Ipswich, MA, USA) was added to the cells immediately after electroporation and the  
173 resuspended cells were incubated with shaking at 200 rpm, 30 °C for one hour. The entire  
174 transformation medium was plated on an LB agar plate containing 50  $\mu$ g/mL kanamycin.  
175 Plasmid transformation was verified by restriction digest and gel electrophoresis.

176

177



178 *Methyl ketone production from purified substrates by P. putida and E. coli*

179 Methyl ketone production assays were conducted in 15-mL test tubes with glucose, xylose, 4-  
180 hydroxybenzoate (4-HB) and protocatechuate (PCA) as carbon sources. Where indicated, the  
181 medium was amended with a mixture of amino acids (serine, valine, aspartate, phenylalanine,  
182 and tryptophan in equal amounts, total concentration was 0.5-1.5 g/L). A single colony of *P.*  
183 *putida* JD4 (*AfadAB*, *ΔphaCZC*, pJM20) was first grown at 30°C in minimal medium with 50  
184 μg/mL kanamycin for ~12 h as the seed culture. The seed culture (5% v/v) was inoculated into  
185 each tube with 10 mL minimal medium. After ~6 h growth at 30 °C, 0.2 % (w/v) of L-arabinose  
186 was added for induction and 2 mL decane overlay was added for methyl ketone extraction. After  
187 48 h, the decane was sampled and methyl ketone production measured using GC-MS (see  
188 below). *E. coli* EGS1895 freezer stock was first activated at 37 °C in M9-MOPS minimal  
189 medium with 50 μg/mL kanamycin for ~12 h as the seed culture. The seed culture (5% v/v) was  
190 inoculated into each tube with 10 mL minimal medium. After ~6 h growing at 37°C, 0.5 mM  
191 IPTG and 1 mM arabinose was added for induction and 2 mL decane overlay was added for  
192 methyl ketone extraction. After 72 h, the decane was sampled and methyl ketone production  
193 measured using GC-MS (see below).

194

195 *Preparation of biomass hydrolysates for methyl ketone production*

196 *Arabidopsis thaliana* (L.) Heynh. ecotype Col-0 wild-type lines and engineered lines modified in  
197 lignin biosynthesis were previously described and grown at the Joint BioEnergy Institute (Eudes  
198 et al., 2012, 2015). Switchgrass (*Panicum virgatum* L., cultivar Alamo) was grown in a chamber  
199 at the Joint BioEnergy Institute under the following conditions: 25 °C, 60% humidity and 14 h of  
200 light per day (250 μmol.m<sup>-2</sup>.s<sup>-1</sup>). Sorghum (*Sorghum bicolor*) was provided by Idaho National

201 Laboratory. Biomass (400 mg) was pretreated in 6.8 mL 1% (w/w) H<sub>2</sub>SO<sub>4</sub> (6% w/w solid  
202 loading) at 121°C 20 psi for 1 h. Phosphate buffer (1 mL; pH 6.2) and distilled water (12 mL)  
203 were added and the pH was adjusted to 5.5 with an equimolar NaOH and KOH solution (5 N).  
204 CTec3 (5 µL, Novozymes) was added to the pH-adjusted slurry and saccharification was  
205 conducted in a VWR hybridization oven (Model 5420) at 15 rpm, 50 °C for 48 h. The pH was  
206 adjusted to 7.2 with equimolar NaOH and KOH solution (5 N) and the combined hydrolysate  
207 was centrifuged at 10,000 *x g* for 20 min and filtered through a 0.2-µm nylon membrane to  
208 remove residual solids. The clear supernatant was stored for 4 °C for further use. To separate the  
209 acid hydrolysate, the slurry obtained after dilute acid pretreatment was centrifuged at 10,000 *x g*  
210 for 20 min and the supernatant, referred to as the acid hydrolysate, stored at 4°C. The remaining  
211 solid was resuspended in 19 mL of distilled water and its pH adjusted to 5.5 with an equimolar  
212 NaOH and KOH solution (5 N). Hydrolysis with CTec3 was performed as described above,  
213 yielding the enzymatic hydrolysate. For methyl ketone production using these enzymatic  
214 hydrolysates, concentrated medium supplements were added into the hydrolysates, as the media  
215 lacked additional carbon sources and buffers (KH<sub>2</sub>PO<sub>4</sub> and Na<sub>2</sub>HPO<sub>4</sub> in *P. putida* medium;  
216 MOPS in *E. coli* medium). The solution was then filtered through a 0.2-µm membrane for  
217 sterilization and the cultivation performed under the same conditions as the pure substrates.

218

### 219 *Proteomics*

220 Samples prepared for shotgun proteomic experiments were analyzed by an Agilent 6550 iFunnel  
221 Q-TOF mass spectrometer (Agilent Technologies, Santa Clara, CA) coupled to an Agilent 1290  
222 UHPLC system as described previously (González Fernández-Niño et al., 2015). Peptides (20  
223 µg) were separated on a Sigma–Aldrich Ascentis Peptides ES-C18 column (2.1 mm × 100 mm,

224 2.7  $\mu\text{m}$  particle size, operated at 60°C) at a 0.40 mL/min flow rate and eluted with the following  
225 gradient: initial condition was 95% solvent A (0.1% formic acid) and 5% solvent B (99.9%  
226 acetonitrile, 0.1% formic acid). Solvent B was increased to 35% over 120 min, and then  
227 increased to 50% over 5 min, then up to 90% over 1 min, and held for 7 min at a flow rate of 0.6  
228 mL/min, followed by a ramp back down to 5% B over 1 min where it was held for 6 min to re-  
229 equilibrate the column to original conditions. Peptides were introduced to the mass spectrometer  
230 from the liquid chromatography (LC) by using a Jet Stream source (Agilent Technologies)  
231 operating in positive-ion mode (3,500 V). Source parameters employed gas temp (250°C), drying  
232 gas (14 L/min), nebulizer (35 psig), sheath gas temp (250°C), sheath gas flow (11 L/min), VCap  
233 (3,500 V), fragmentor (180 V), OCT 1 RF Vpp (750 V). The data were acquired with Agilent  
234 MassHunter Workstation Software, LC/MS Data Acquisition B.06.01 operating in Auto MS/MS  
235 mode whereby the 20 most intense ions (charge states, +2–5) within 300–1,400  $m/z$  mass range  
236 and above a threshold of 1,500 counts were selected for MS/MS analysis. MS/MS spectra (100–  
237 1,700  $m/z$ ) were collected with the quadrupole set to “Medium” resolution and were acquired  
238 until 45,000 total counts were collected or for a maximum accumulation time of 333 ms. Former  
239 parent ions were excluded for 0.1 min following MS/MS acquisition. The acquired data were  
240 exported as mgf files and searched against the latest *P. putida* KT2440 protein database  
241 supplemented with coding protein sequences in the TOL plasmid with Mascot search engine  
242 version 2.3.02 (Matrix Science). The chromosomal genome of *P. putida* KT2440 and *P. putida*  
243 mt-2 are identical . The resulting search results were filtered and analyzed by Scaffold v 4.3.0  
244 (Proteome Software Inc.). A total of 876 proteins were found that had at least two peptides  
245 identified with 95% confidence in at least one of the biological replicates. The normalized  
246 spectral counts of identified proteins were exported for relative quantitative analysis.

247 *Analysis*

248 Concentrations of organic compounds except for amino acids in the media or hydrolysates were  
249 measured with an Agilent 1100 Series HPLC system equipped with an Agilent 1200 Series  
250 refractive index detector (RID) and diode array and multiple wavelength detector (DAD)  
251 (Agilent Technologies) (Goh et al., 2014). Aliquots (1 mL) of cell cultures were collected and  
252 centrifuged. The supernatants were filtered through a spin-cartridge with a 0.45- $\mu$ m nylon  
253 membrane. For glucose and xylose detection, 5- $\mu$ L samples were eluted through Aminex HPX-  
254 87H ion-exclusion column (300-mm length, 7.8-mm internal diameter; Bio-Rad Laboratories,  
255 Inc.) at 50 °C with 4 mM sulfuric acid at a flow rate of 600  $\mu$ L/min for 15 min. Glucose and  
256 xylose were detected by RID. For 4-HB and PCA detection, 5  $\mu$ L was eluted through Hypersil  
257 ODS C18 column (250-mm length, 4.6-mm internal diameter; Thermo Fisher Scientific) at 20°C  
258 with 20% (v/v) acetonitrile and 0.5% (v/v) acetic acid in water at a flow rate of 900  $\mu$ L/min for  
259 15 min. PCA and 4-HB were detected by DAD at 275 nm (Heinaru et al., 2001).

260

261 Methyl ketones present in the decane overlay were quantified using electron-ionization gas  
262 chromatography/mass spectrometry (GC/MS) as described previously (Goh et al., 2012). For the  
263 measurement of amino acids in hydrolysates, liquid chromatographic separation was conducted  
264 using a Kinetex HILIC column (100-mm length, 4.6-mm internal diameter, 2.6- $\mu$ m particle size;  
265 Phenomenex, Torrance, CA) using a 1200 Series HPLC system (Agilent Technologies, Santa  
266 Clara, CA, USA). The injection volume for each measurement was 2  $\mu$ L. The sample tray and  
267 column compartment were set to 6°C and 40°C, respectively. The mobile phase was composed  
268 of 20 mM ammonium acetate in water (solvent A) and 10 mM ammonium acetate in 90%  
269 acetonitrile and 10% water (solvent B) (HPLC grade, Honeywell Burdick & Jackson, CA, USA).

270 Ammonium acetate was prepared from a stock solution of 100 mM ammonium acetate and 0.7 %  
271 formic acid (98-100% chemical purity, from Sigma-Aldrich, St. Louis, MO, USA) in water.  
272 Amino acids were separated with the following gradient: 90% to 70%B in 4 min, held at 70%B  
273 for 1.5 min, 70% to 40%B in 0.5 min, held at 40%B for 2.5 min, 40% to 90%B in 0.5 min, held  
274 at 90%B for 2 min. The flow rate was varied as follows: held at 0.6 mL/min for 6.5 min, linearly  
275 increased from 0.6 mL/min to 1 mL/min in 0.5 min, and held at 1 mL/min for 4 min. The total  
276 run time was 11 min. The mass spectrometry parameters have been previously described  
277 (Bokinsky et al., 2013).

278

#### 279 *Strain and Data Availability*

280 Strains are available from the JBEI Public Registry (<https://public-registry.jbei.org/>) and the IDs  
281 are listed in Table 1. The mass spectrometry proteomics data have been deposited to the  
282 ProteomeXchange Consortium via the PRIDE partner repository (Vizcaíno et al., 2016) with the  
283 dataset identifier PXD012013 and 10.6019/PXD01201.

284

285

## 286 **RESULTS**

### 287 *Engineering P. putida for methyl ketone production*

288 A successful strategy for microbial production of methyl ketones (C<sub>11</sub>-C<sub>15</sub>) is to prevent native  $\beta$ -  
289 oxidation, deregulate fatty acid biosynthesis and express a truncated  $\beta$ -oxidation pathway to  
290 form  $\beta$ -keto-acids, which spontaneously decarboxylate to methyl ketones (Goh et al., 2012) . For  
291 *P. putida*, previous work has demonstrated that the deletion of *fadAB* and genes for PHA  
292 polymerization (*phaC*) prevented  $\beta$ -oxidation of fatty acids and overproduced  $\beta$ -hydroxy-acids,  
293 which are thiolitic products of  $\beta$ -hydroxyacyl-CoAs and key intermediates in methyl ketone  
294 production (Ouyang, Luo, et al., 2007). Therefore, both *fadAB* and the PHA synthase *pha* operon  
295 (*phaC1-phaZ-phaC2*) were deleted to eliminate competition for the hydroxyacyl-CoA  
296 intermediates. Four genes (*tesA*, *Mlut\_11700*, *fadB* and *fadM*) were transformed into *P. putida*  
297 mt-2 on a pBBR1-MCS2-based broad host plasmid under the control of P<sub>BAD</sub> (Müller et al.,  
298 2013). *E. coli tesA* encodes for a thioesterase with a truncated leader sequence that deregulates  
299 fatty acid biosynthesis by thiolysis of acyl-CoAs and acyl-ACPs. *Mlut\_11700* encodes for a  
300 soluble acyl-CoA oxidase from *Micrococcus luteus*. *E. coli FadB* converts the enoyl-CoAs  
301 produced by the acyl-CoA oxidase to  $\beta$ -keto-acyl-CoAs, which are converted to  $\beta$ -keto acids by  
302 the *E. coli* thioesterase FadM. The spontaneous decarboxylation of  $\beta$ -keto acids produces methyl  
303 ketones through a non-enzymatic process (Goh et al., 2014).

304

### 305 *Methyl ketone production by P. putida*

306 The production of methyl ketones was tested with either glucose or lignin-related aromatics as  
307 the sole carbon source in minimal medium. Two aromatics, 4-hydroxybenzoate (4-HB) and

308 protocatechuate (PCA), were also tested as carbon sources since these aromatics accumulated in  
309 engineered *Arabidopsis* plants whose hydrolysates we planned on testing for methyl ketone  
310 production (Eudes et al., 2012)(Eudes et al., 2015). *P. putida* JD4, which contained the deletions  
311 in the PHA synthesis and  $\beta$ -oxidation pathways, produced >200 mg/L of methyl ketones from  
312 glucose and ~300 mg/L from 4-HB. PCA was a poor substrate for methyl ketone production,  
313 producing <30 mg/L from the combined mutant, which may arise due to chelation of the  $Fe^{2+}$   
314 present in the medium by PCA (Kamariotaki et al., 1994) (Gerega et al., 1987) (**Figure 1**). The  
315 chelation complex may hinder growth by reducing the availability of PCA or directly inhibiting  
316 *P. putida* and was therefore not tested in the other deletion strains. *P. putida* JD5, which has a  
317 deletion of *fadAB*, resulted in the production of 140-150 mg/L methyl ketones from glucose and  
318 4-HB (**Figure S1**). *P. putida* JD6, which has the lesion in the PHA synthesis genes, only  
319 produced methyl ketones from 4-HB, which may arise from a reduced flux of aromatic substrates  
320 to PHA synthesis compared to glucose (Linger et al., 2014). The most abundant methyl ketones  
321 produced in *P. putida* were C<sub>13</sub> and C<sub>15</sub> methyl ketones, which is similar in chain length to *R.*  
322 *eutropha* (Müller et al., 2013) and *E. coli* (Goh et al., 2012). The majority of the methyl ketones  
323 (>60%) were unsaturated suggesting that they were converted from a high portion of unsaturated  
324 fatty acids produced in *P. putida*.

325

### 326 *Methyl ketone production from engineered Arabidopsis thaliana*

327 Methyl ketone production with single substrates provided background for experiments that tested  
328 production with plant hydrolysates. As noted above, we chose hydrolysates from *A. thaliana*  
329 lines in which lignin biosynthesis was disrupted by the expression of bacterial genes. Two  
330 strategies were pursued in *A. thaliana* to disrupt lignin biosynthesis, which lowered plant lignin

331 content and improved polysaccharide hydrolysis. In the first strategy, expression of 3-  
332 dehydroshikimate dehydratase (QsuB from *C. glutamicum*) converts 3-dehydroshikimate, an  
333 important intermediate in lignin synthesis, into PCA (Eudes et al., 2015). In the second strategy  
334 hydroxycinnamoyl-CoA hydratase-lyase (HCHL) from *Pseudomonas fluorescens* AN103 was  
335 expressed to reroute the lignin biosynthetic intermediate *p*-coumaroyl-CoA into 4-  
336 hydroxybenzaldehyde, which was further oxidized to 4-HB (Eudes et al., 2012). The PCA-  
337 producing *A. thaliana* line is subsequently referred to as the QsuB line and the 4-HB-producing  
338 line is referred to as the HCHL line.

339  
340 A mild acid pretreatment of biomass from these engineered plants followed by enzymatic  
341 hydrolysis was developed to produce hydrolysates that contained both sugars and aromatics. The  
342 two *A. thaliana* lines released more sugars, especially glucose, compared to wild type control  
343 plants, (**Figure 2A**). Hydrolysates from the QsuB line contained ~1.0 g/L of PCA (~5% of dry  
344 biomass) and those from HCHL line had ~ 0.2 g/L of 4-HB (~1% of dry biomass). Although the  
345 *A. thaliana* biomass also generates ~2.0 g/L xylose, primarily by acid hydrolysis, *P. putida* mt-2  
346 cannot metabolize xylose into TCA cycle. Incubations with glucose and xylose demonstrated  
347 >90% conversion of xylose to xylonate, which was not further incorporated (data not shown).  
348 The near quantitative production of xylose from xylonate has previously been observed in *P.*  
349 *putida* S12 (Meijnen, de Winde, & Ruijssenaars, 2008).

350  
351 The growth and methyl ketone production using these *A. thaliana* hydrolysates as carbon  
352 sources were tested. *P. putida* reached higher optical densities in the cultures grown with  
353 hydrolysates from the QsuB and HCHL lines compared to those grown with hydrolysates



354 obtained from the corresponding wild type control plants, likely because of the increased  
355 concentration of glucose in these hydrolysates (**Figure S2A**). Surprisingly, all the *A. thaliana*  
356 hydrolysates produced higher levels of methyl ketones than the sugar-only controls (**Figure 2B**).  
357 Hydrolysates from wild type and QsuB plants provided 2-3 fold higher methyl ketone than the  
358 glucose/xylose control, which suggested that other components in the plant hydrolysates  
359 increased methyl ketone titers. The hydrolysate from the HCHL plants gave the highest methyl  
360 ketone titer (~ 500 mg/L), which is ~2x the titer achieved with hydrolysates from wild type  
361 plants and ~ 5x the titer of the sugar-only control.

362  
363 Methyl ketone production with *P. putida* was compared to an *E. coli* strain (*E. coli* EGS1895)  
364 optimized for methyl ketone production from glucose by improving flux through the fatty acid  
365 pathway and eliminating acetate production; these modifications to the base strain, which  
366 focused on truncating  $\beta$ -oxidation, demonstrated >1g/L of methyl ketone production from 1%  
367 glucose in M9 minimal medium (Goh et al., 2014). As with the *P. putida* cultures, *E. coli*  
368 GS1895 reached higher optical density in the cultures grown with hydrolysates from the *A.*  
369 *thaliana* QsuB and HCHL lines (**Figure S2B**). *E. coli* EGS1895 displayed high levels of methyl  
370 ketone production (1.3 g/L) in cultures with the glucose/xylose control, but *E. coli*'s methyl  
371 ketone titers using *A. thaliana* hydrolysates were only 40%-60% of the control. As with *P.*  
372 *putida*, cultures grown on hydrolysates from biomass of the *A. thaliana* HCHL line produced the  
373 highest concentration of methyl ketones among the hydrolysate-fed cultures (~800 mg/L)  
374 (**Figure 2C**).

375

376

377 *Methyl ketones production from switchgrass*

378 The attenuation of methyl ketone production by *E. coli* when grown on plant hydrolysates was  
379 not surprising based on previous studies demonstrating inhibition by plant hydrolysates;  
380 however, the large increase in titer compared to sugar only controls for *P. putida* was  
381 unexpected. To investigate further if the high methyl ketone production from hydrolysates was  
382 unique to *A. thaliana*, we tested hydrolysates obtained from switchgrass. Switchgrass has been  
383 shown to be a source of hydrolysates for biological conversion to a variety of biofuels and bio-  
384 based chemicals (Bokinsky et al., 2011). Mild dilute acid pretreatment and enzymatic hydrolysis  
385 yielded ~ 5.0 g/L of glucose and ~ 4.0 g/L of xylose in the combined hydrolysate (**Figure 3A**). In  
386 a second pretreatment, the solid was separated from the acid hydrolysate and subsequently  
387 hydrolyzed with enzymes, producing a separate enzymatic hydrolysate. The acid hydrolysate  
388 contained mainly xylose (~ 3.5 g/L) and small amount of glucose (~ 0.8 g/L), while glucose (~  
389 3.5 g/L) predominated in the enzymatic hydrolysate with a small amount of xylose (~ 0.8 g/L).

390

391 Methyl ketone production by *P. putida* JD4 was tested in cultures with the combined and  
392 separated switchgrass hydrolysates. Growth, as measured by OD<sub>600</sub>, was better in the cultures  
393 with the combined hydrolysate compared to the sugar only control (**Figure S3A**). Final ODs  
394 were similar in the cultures grown on each of the separated switchgrass hydrolysates, and were  
395 ~50% higher than those attained with the sugar-only control. Methyl ketone production from the  
396 combined switchgrass hydrolysate was >7-fold higher (710 mg/L versus 92 mg/L) in the  
397 combined hydrolysate compared to the sugar control (**Figure 3B**). The separated switchgrass  
398 hydrolysates produced substantially lower titer of methyl ketones, with the acid hydrolysate (170  
399 mg/L) producing higher concentrations than the enzymatic hydrolysate (70 mg/L), despite having

400 ~4.5-fold less glucose in the acid hydrolysate. The comparison of *P. putida* methyl ketone  
401 production from the combined and separated switchgrass hydrolysates suggested that the high  
402 relative methyl ketone titer obtained for the combined hydrolysate arose from synergistic  
403 interactions between components of the acid and enzymatic hydrolysate.

404

405 Complementary methyl ketone production experiments using the same combined and separated  
406 switchgrass hydrolysates were performed with *E. coli* EGS1895. OD measurements indicated  
407 that both the combined and acid hydrolysates promoted better growth than the sugar-only control  
408 (**Figure S3B**). In contrast, the enzymatic switchgrass hydrolysate supported lower levels of  
409 growth than the sugar controls (OD ~60% of the control). As with the *A. thaliana* hydrolysates,  
410 *E. coli* EGS1895 produced lower concentrations of methyl ketones from the combined  
411 hydrolysate compared to the sugar control. In contrast to *P. putida*, the enzymatic switchgrass  
412 hydrolysate yielded more methyl ketone (550 mg/L) compared to the acid hydrolysate (220  
413 mg/L) and the sum was greater than the production achieved with the combined switchgrass  
414 hydrolysate (700 mg/L), which suggests that there were negative interactions between the  
415 components of the acid and enzymatic hydrolysate during *E. coli* conversion of the methyl  
416 ketones (**Figure 3C**).

417

418 *Proteomics*

419

420 Global proteomic analysis *P. putida* JD4 grown either on hydrolysates from biomass of HCHL  
421 line and switchgrass or on glucose-rich control medium was performed to identify the  
422 determinants of increased production with these different substrates. Three of the four proteins  
423 that constitute the methyl ketone production pathway (*E. coli* FadM, FadB and TesA) were  
424 among the top 50 proteins present at highest abundance in the *P.putida* JD4 proteome and were

425 2-3 fold more abundant in the cultures grown on the HCHL and switchgrass hydrolysates  
426 (**Figure 4**) (**Table S1**). The abundance of the *M. luteus* acyl-CoA oxidase encoded by  
427 *Mlut\_11700* was comparable in all the cultures. A native long chain acyl-CoA dehydrogenase  
428 (FadE), which catalyzes the same transformation as the acyl-CoA oxidase, was present at higher  
429 abundance in the cultures from switchgrass hydrolysate after 24 h and in the cultures from both  
430 the HCHL and switchgrass hydrolysates after 48 h. This protein has previously been  
431 characterized as a phenylacyl-CoA dehydrogenase, but can also accept C<sub>14</sub> and C<sub>16</sub> acyl-CoAs  
432 (McMahon & Mayhew, 2007). FadH, a 2,4-dienoyl-CoA reductase, was present at 3-to-6 fold  
433 higher levels in the hydrolysate cultures. This protein has not been characterized in *P. putida*, but  
434 functions as a reductase for polyunsaturated acyl-CoA molecules in *E. coli* (You, Cosloy, &  
435 Schulz, 1989). The high abundance of FadH suggests that the  $\beta$ -oxidation of unsaturated fatty  
436 acids is a key step in methyl ketone production. Small but significant increases in abundance  
437 were observed for proteins involved in fatty acid biosynthesis (AccA, AccB, FabD, FabV, FabG,  
438 FabB), which are consistent with the observation of increased flux through the fatty acid  
439 biosynthesis pathway.

440

441 Proteins involved in amino acid catabolism were more abundant in the proteomes from the  
442 cultures obtained from plant hydrolysate compared to those grown only from glucose (Table S2).  
443 Proteins for arginine catabolism: ArcA (arginine deaminase), ArcB (ornithine decarboxylase)  
444 and ArcC (carbamate kinase) were present at higher abundances in both cultures from  
445 hydrolysate, with the ArcA protein present at ~3 fold higher levels using the *A. thaliana*  
446 hydrolysate. For the culture grown on switchgrass hydrolysate, a glutaminase-asparaginase was  
447 present at 4-fold higher levels at 24 h compared to the control culture grown from sugar only. In

448 addition, proteins involved in aromatic amino acid catabolism, including:  
449 hydroxyphenylpyruvate dioxygenase, homogentisate dioxygenase (HmgA), and  
450 fumarylacetoacetate hydrolase (HmgB) were present at higher levels in cultures obtained from  
451 the switchgrass hydrolysate.

452

453 The proteomic analysis also indicated that other cell wall components besides glucose and xylose  
454 were metabolized by *P. putida* in the plant hydrolysates (**Table S3**). Proteins involved in  
455 aromatic catabolic pathways were only detected in cultures conducted with the plant  
456 hydrolysates. 4-HB hydroxylase, which convert 4-HB to PCA, was present at higher levels in  
457 cultures from HCHL hydrolysate, which was consistent with the increased production of 4-HB in  
458 the *A. thaliana* HCHL line. Some of the downstream proteins involved in PCA conversion to 3-  
459 oxoadipate (PcaH, PcaI) were detected in the proteome, albeit at relatively low abundances.  
460 Vanillin dehydrogenase (vdh) and enoyl-CoA hydratase/aldoase, which is involved in ferulate  
461 catabolism, were detected at higher abundances in the culture from switchgrass hydrolysates,  
462 which reflects the presence of low concentrations of aromatics released by the dilute acid  
463 pretreatment and enzymatic hydrolysis (**Table 2**).

464

465 *Correlation between amino acid in hydrolysates and methyl ketone production*

466

467 The elevated levels of amino acid catabolic proteins detected by proteomics for *P. putida*  
468 cultivated in the *A. thaliana* HCHL and switchgrass hydrolysates suggested that plant-derived  
469 amino acids were critical contributors to the increased methyl ketone titers in plant hydrolysates.  
470 Control experiments adding 4-HB to the glucose/xylose control medium did not greatly enhance  
471 the methyl ketone production. Inclusion of acetate, present in all the hydrolysates, also did not

472 increase methyl ketone production (**Figure S4**). The concentrations of glucose, the primary  
473 substrate for *P. putida*, and arabinose, the inducer for methyl ketone production, were not  
474 correlated with methyl ketone production. LC-MS measurements demonstrated that the  
475 switchgrass hydrolysate contained the highest concentrations of amino acids (~1.16 g/L) of plant  
476 hydrolysates tested for methyl ketone production (**Figure 5A**). The *A. thaliana* HCHL  
477 hydrolysate had ~0.85 g/L total amino acids while the *A. thaliana* QsuB hydrolysates and the  
478 wild-type hydrolysates had 0.2-0.4 g/L of amino acids (**Table 2**). The amino acid profiles from  
479 different biomass shared some common features; the most abundant amino acids in all the  
480 hydrolysates were serine, valine, aspartate, phenylalanine and tryptophan. The switchgrass  
481 hydrolysate was enriched in aspartate (~0.45 g/L), accounting for the overall increase in amino  
482 acid concentration relative to the *A. thaliana* hydrolysates. As validation of this proposed  
483 correlation between plant-derived amino acids and methyl ketone production, a sorghum  
484 hydrolysate was generated using mild acidic conditions and it contained 0.4 g/L of amino acids  
485 with 3.5 g/L of glucose and 2.4 g/l xylose. Incubation of the sorghum hydrolysate with *P. putida*  
486 JD3 produced 400 mg/L of methyl ketones, which was consistent with the excellent linear  
487 correlation between methyl ketone production and amino acid concentrations for the plant  
488 hydrolysates (**Figure 5B**).

489

#### 490 *Amino acid-amended medium improves P. putida methyl ketone production*

491 Experiments with plant hydrolysates described above provided evidence that the presence of  
492 plant-derived amino acids, produced by acid hydrolysis of the biomass, significantly contributed  
493 to the overall increase in methyl ketone production. These results suggested that amending the  
494 minimal medium used to produce methyl ketones with amino acids would also increase methyl

495 ketone production. A mixture of the five most abundant amino acids found in the hydrolysates  
496 (serine, valine, aspartate, phenylalanine and tryptophan in equal amounts) was added into  
497 minimal medium containing glucose (5 g/L). In the absence of glucose, the amino acid mixture  
498 was able to support growth and methyl ketone production (193 mg/L at 1.5 g/L amino acids).  
499 The addition of glucose resulted in a substantial increase in methyl ketone production (300 mg/L  
500 at 0.5 g/L amino acids; 1.1 g/L at 1.5 g/L amino acids) (**Figure 6**), which represented a ~9-fold  
501 increase relative to the glucose-only control when MK production from the amino acids was  
502 subtracted.

503

504 **DISCUSSION**

505 This work was initiated to develop microbial hosts for biofuel and bio-based chemical  
506 production that could convert both sugars and aromatics in plant hydrolysates. Here we show  
507 that common pretreatment and saccharification protocols (mild acid hydrolysis, combining acid  
508 and enzymatic hydrolysates), which generated hydrolysates containing sugars, aromatics, and  
509 amino acids, substantially increased production of fatty acid-derived methyl ketones in an  
510 engineered *P. putida* strain.

511  
512 Engineered *P. putida* mt-2 strains produced C<sub>13</sub> and C<sub>15</sub> methyl ketones when grown on both  
513 glucose and aromatic substrates. The methyl ketone products were highly enriched in unsaturated  
514 methyl ketones (>60% C<sub>13:1</sub> and C<sub>15:1</sub>). In *E. coli*, the C<sub>13:0</sub> chain was the most abundant methyl  
515 ketone, but there was a substantial proportion of C<sub>13:1</sub> and C<sub>15:1</sub> ketones (Goh et al., 2012). In  
516 contrast, *R. eutropha* produced C<sub>13:0</sub> and C<sub>15:0</sub> at >90% of the total methyl ketone fraction  
517 (Müller et al., 2013). Interestingly, the most abundant chain in the membrane fatty acid  
518 composition of *P. putida* mt-2 is C<sub>16:0</sub> (Hachicho, Birnbaum, & Heipieper, 2017), which suggests  
519 that the pool of acyl-CoA intermediates that is diverted to methyl ketone production differs from  
520 the ACP intermediates that are converted to membrane lipids in *P. putida*. The increase in  
521 unsaturated methyl ketones may arise because of cellular stress response, as has been observed  
522 for fatty acid production by *E. coli* (Lennen et al., 2011). Additionally, the chain length  
523 distribution differs from *mcl*-PHAs produced by *P. putida* KT2440, which has the same  
524 chromosomal genotype as *P. putida* mt-2 but lacks the TOL plasmid, when the *phaC* genes are  
525 not deleted. *P. putida* KT2440 produced *mcl*-PHAs in which hydroxydecanoate monomers  
526 predominated (>50%) when grown on glucose or lignin-related aromatics (*p*-coumarate, ferulate)



527 (Linger et al., 2014)The monomer distribution of *mcl*-PHAs in *P. putida* grown on non-fatty acid  
528 substrates is highly dependent by PhaG, a transacylase that converts ACP thioesters to acyl-  
529 CoAs and is specific for 3-hydroxydecanoate. Further studies on fatty acid biosynthesis and  $\beta$ -  
530 oxidation in *P. putida* are needed to establish the basis for the distribution of methyl ketone  
531 products and account for their differences compared to membrane fatty acids and *mcl*-PHA  
532 monomers.

533

534 Pretreatment of lignocellulosic biomass often generates inhibitors that limit growth and lower  
535 product titers and rates relative to those obtained using glucose-containing defined media. This  
536 loss of productivity has been observed in the production of succinate from corn stover dilute acid  
537 hydrolysate by *Actinobacillus succinogenes* (Salvachúa et al., 2016) and fatty alcohol production  
538 from ionic liquid pretreated switchgrass by *Saccharomyces cerevisiae* (Espaux et al., 2017). In  
539 particular, dilute acid hydrolysates contain a variety of inhibitors, including phenolics, acetate  
540 and furfural, that have been shown to inhibit a variety of hosts for biofuel and biochemical  
541 production (Larsson et al., 1999). This phenomenon was observed in this work with the *E. coli*  
542 strain that had been engineered for high yield methyl ketone production from glucose. This *E.*  
543 *coli* strain (EGS1895), displayed methyl ketone titers with plant hydrolysates that were 30-60%  
544 of the titers obtained for sugar-only controls, consistent with the inhibitory effect of these  
545 hydrolysates on bioproduct production. This inhibitory effect on *E. coli* was further supported by  
546 the observation that combining the switchgrass acid and enzymatic hydrolysates lowered the  
547 methyl ketone titer relative to the sum of the individual hydrolysates indicating a negative  
548 synergistic effect (~1.2-fold). *P. putida* strains have demonstrated levels of tolerance to  
549 xenobiotic compounds and oxidative stress, so would be expected to respond more favorably to

550 acid hydrolysates than *E. coli*. However, the enhancing effect of plant hydrolysates on *P. putida*  
551 methyl ketone production, exemplified by the positive synergy (~3-fold) between the switchgrass  
552 acid and enzymatic hydrolysates, indicated that unidentified components were contributing to the  
553 methyl ketone production.

554

555 Mass spectrometry-based proteomics identified amino acid catabolic proteins at higher levels in  
556 the two *P. putida* cultures from plant hydrolysates (*A. thaliana* HCHL and switchgrass) that were  
557 consistent with increased amino acid catabolism. Proteomics indicated higher protein levels of  
558 most of the gene products involved in fatty acid biosynthesis, especially the heterologous  
559 proteins in the methyl ketone pathway, which is consistent with a higher flux toward the fatty  
560 acid pathway. The correlation between amino acid content in hydrolysates and methyl ketone  
561 production, as well as the increase in methyl ketone production in minimal medium  
562 supplemented with amino acid strongly supported the assignment of amino acids as the key  
563 stimulative components in the hydrolysates.

564

565 The effect of amino acids in plant hydrolysates on microbial performance for bioconversion of  
566 lignocellulose is underexplored. The growth of an ethanogenic *E. coli* strain on AFEX-  
567 pretreated corn stover hydrolysate was dependent on the presence of amino acids in the  
568 hydrolysate, and depletion of these amino acids resulted in a transition to stationary phase. This  
569 transition was attributed to an increased requirement for ATP production in the absence of  
570 exogenous amino acids (Schwalbach et al., 2012). Potential bioenergy crops traditionally used  
571 for forage, such as switchgrass, reed canary grass and alfalfa, have high protein content (5-15%)  
572 (Dien et al., 2006) and strategies that integrate amino acid and sugar conversion for hydrolysates

573 derived from these crops may increase the overall efficiency of the biomass to biofuels and  
574 biochemicals. This strategy provides a complement to integrating sugar and aromatic metabolism  
575 for bioconversion that was the impetus for this study. In both scenarios, *P. putida* is a promising  
576 host for bioconversion that possesses capabilities lacking in a widely used host such as *E. coli*.

577

578

579

580

581 **CONCLUSION**

582

583 *P. putida* was successfully engineered to produce C<sub>13</sub> and C<sub>15</sub> methyl ketones from glucose and

584 lignin-related aromatics, 4-HB and PCA. Methyl ketone production by *P. putida* with *A. thaliana*

585 and switchgrass hydrolysates obtained by dilute acid pretreatment led to the identification of

586 plant-derived amino acids, rather than mono-aromatics, as key enhancing components of these

587 hydrolysates. Shotgun proteomics indicated that the amino acids had a specific inductive effect

588 on proteins involved in fatty acid biosynthesis, leading to a 9-fold increase in methyl ketone titer

589 by amending glucose-containing minimal medium with a defined set of amino acids. This work

590 establishes that the unique metabolic capabilities of *P. putida* are suited to produce high levels of

591 fatty acid-derived biofuels and that proteins in plant biomass may be a promising source of

592 amino acids that increase the conversion efficiency of biomass to biofuels and bio-based

593 chemicals.

594

595

596 **ACKNOWLEDGEMENTS**

597

598 This work was performed as part of the DOE Joint BioEnergy Institute (<http://www.jbei.org>)

599 supported by the U.S. Department of Energy, Office of Science, Office of Biological and

600 Environmental Research, through contract DE-AC02-05CH11231 between Lawrence Berkeley

601 National Laboratory and the U.S. Department of Energy. U.S. Government retains and the

602 publisher, by accepting the article for publication, acknowledges that the U.S. Government

603 retains a nonexclusive, paid up, irrevocable, worldwide license to publish or reproduce the

604 published form of this work, or allow others to do so, for U.S. Government purposes.

605

606 **CONFLICT OF INTEREST**

607

608 There are no conflicts of interest to declare.

609 **REFERENCES**

- 610
- 611 Andreoni, V., Bernasconi, S., Bestetti, P., & Villa, M. (1991). Metabolism of Lignin-Related  
612 Compounds by *Rhodococcus rhodochrous* - Bioconversion of Anisoin. *Applied*  
613 *Microbiology and Biotechnology*, 36(3), 410–415.
- 614
- 615 Beckham, G. T., Johnson, C. W., Karp, E. M., Salvachúa, D., & Vardon, D. R. (2016).  
616 Opportunities and challenges in biological lignin valorization. *Current Opinion in*  
617 *Biotechnology*, 42, 40–53. doi:10.1016/j.copbio.2016.02.030
- 618
- 619 Beller, H. R., Lee, T. S., & Katz, L. (2015). Natural products as biofuels and bio-based  
620 chemicals: fatty acids and isoprenoids. *Natural Product Reports*, 32(10), 1508–1526.  
621 doi:10.1039/c5np00068h
- 622
- 623 Bokinsky, G., Baidoo, E. E. K., Akella, S., Burd, H., Weaver, D., Alonso-Gutierrez, J., ...  
624 Keasling, J. D. (2013). HipA-triggered growth arrest and  $\beta$ -lactam tolerance in  
625 *Escherichia coli* are mediated by RelA-dependent ppGpp synthesis. *Journal of*  
626 *Bacteriology*, 195(14), 3173–3182. doi:10.1128/JB.02210-12
- 627
- 628 Bokinsky, G., Peralta-Yahya, P. P., George, A., Holmes, B. M., Steen, E. J., Dietrich, J., ...  
629 Keasling, J. D. (2011). Synthesis of three advanced biofuels from ionic liquid-pretreated  
630 switchgrass using engineered *Escherichia coli*. *Proceedings of the National Academy of*  
631 *Sciences of the United States of America*, 108(50), 19949–19954.  
632 doi:10.1073/pnas.1106958108
- 633
- 634 Bugg, T. D. H., Ahmad, M., Hardiman, E. M., & Singh, R. (2011). The emerging role for  
635 bacteria in lignin degradation and bio-product formation. *Current Opinion in*  
636 *Biotechnology*, 22(3), 394–400. doi:10.1016/j.copbio.2010.10.009
- 637
- 638 Choi, K.-H., & Schweizer, H. P. (2005). An improved method for rapid generation of unmarked  
639 *Pseudomonas aeruginosa* deletion mutants. *BMC Microbiology*, 5, 30. doi:10.1186/1471-  
640 2180-5-30
- 641
- 642 Dien, B., Jung, H., Vogel, K., Casler, M., Lamb, J., Iten, L., ... Sarath, G. (2006). Chemical  
643 composition and response to dilute-acid pretreatment and enzymatic saccharification of  
644 alfalfa, reed canarygrass, and switchgrass. *Biomass and Bioenergy*, 30(10), 880–891.  
645 doi:10.1016/j.biombioe.2006.02.004
- 646
- 647 Espaux, L. d', Ghosh, A., Rungtaphan, W., Wehrs, M., Xu, F., Konzock, O., ... Keasling, J. D.  
648 (2017). Engineering high-level production of fatty alcohols by *Saccharomyces cerevisiae*  
649 from lignocellulosic feedstocks. *Metabolic Engineering*, 42, 115–125.  
650 doi:10.1016/j.ymben.2017.06.004
- 651
- 652 Eudes, A., George, A., Mukerjee, P., Kim, J. S., Pollet, B., Benke, P. I., ... Loqué, D. (2012).  
653 Biosynthesis and incorporation of side-chain-truncated lignin monomers to reduce lignin  
654 polymerization and enhance saccharification. *Plant Biotechnology Journal*, 10(5), 609–

- 655 620. doi:10.1111/j.1467-7652.2012.00692.x
- 656 Eudes, A., Sathitsuksanoh, N., Baidoo, E. E. K., George, A., Liang, Y., Yang, F., ... Loqué, D.  
657 (2015). Expression of a bacterial 3-dehydroshikimate dehydratase reduces lignin content  
658 and improves biomass saccharification efficiency. *Plant Biotechnology Journal*, 13(9),  
659 1241–1250. doi:10.1111/pbi.12310
- 660
- 661 Fiorentino, G., Ripa, M., & Ulgiati, S. (2017). Chemicals from biomass: technological versus  
662 environmental feasibility. A review. *Biofuels, Bioproducts and Biorefining*, 11(1), 195–  
663 214. doi:10.1002/bbb.1729
- 664
- 665 Gerega, K., Kozłowski, H., Kiss, T., Micera, G., Strinna Erre, L., & Cariati, F. (1987). Cupric  
666 complexes with 3,4-dihydroxybenzoic acid. *Inorganica Chimica Acta*, 138(1), 31–34.  
667 doi:10.1016/S0020-1693(00)81177-9
- 668
- 669 Goh, E.-B., Baidoo, E. E. K., Burd, H., Lee, T. S., Keasling, J. D., & Beller, H. R. (2014).  
670 Substantial improvements in methyl ketone production in *E. coli* and insights on the  
671 pathway from in vitro studies. *Metabolic Engineering*, 26, 67–76.  
672 doi:10.1016/j.ymben.2014.09.003
- 673
- 674 Goh, E.-B., Baidoo, E. E. K., Keasling, J. D., & Beller, H. R. (2012). Engineering of bacterial  
675 methyl ketone synthesis for biofuels. *Applied and Environmental Microbiology*, 78(1),  
676 70–80. doi:10.1128/AEM.06785-11
- 677
- 678 Goh, E.-B., Chen, Y., Petzold, C. J., Keasling, J. D., & Beller, H. R. (2018). Improving methyl  
679 ketone production in *Escherichia coli* by heterologous expression of NADH-dependent  
680 FabG. *Biotechnology and Bioengineering*, 115(5), 1161–1172. doi:10.1002/bit.26558
- 681
- 682 González Fernández-Niño, S. M., Smith-Moritz, A. M., Chan, L. J. G., Adams, P. D.,  
683 Heazlewood, J. L., & Petzold, C. J. (2015). Standard flow liquid chromatography for  
684 shotgun proteomics in bioenergy research. *Frontiers in Bioengineering and*  
685 *Biotechnology*, 3, 44. doi:10.3389/fbioe.2015.00044
- 686
- 687 Hachicho, N., Birnbaum, A., & Heipieper, H. J. (2017). Osmotic stress in colony and planktonic  
688 cells of *Pseudomonas putida* mt-2 revealed significant differences in adaptive response  
689 mechanisms. *AMB Express*, 7(1), 62. doi:10.1186/s13568-017-0371-8
- 690
- 691 Hanko, E. K. R., Denby, C. M., Sánchez I Nogué, V., Lin, W., Ramirez, K. J., Singer, C. A., ...  
692 Keasling, J. D. (2018). Engineering  $\beta$ -oxidation in *Yarrowia lipolytica* for methyl ketone  
693 production. *Metabolic Engineering*, 48, 52–62. doi:10.1016/j.ymben.2018.05.018
- 694
- 695 Heinaru, E., Viggor, S., Vedler, E., Truu, J., Merimaa, M., & Heinaru, A. (2001). Reversible  
696 accumulation of p-hydroxybenzoate and catechol determines the sequential  
697 decomposition of phenolic compounds in mixed substrate cultivations in pseudomonads.  
698 *FEMS Microbiology Ecology*, 37(1), 79–89. doi:10.1111/j.1574-6941.2001.tb00855.x
- 699
- 700 Johnson, C. W., & Beckham, G. T. (2015). Aromatic catabolic pathway selection for optimal

- 701 production of pyruvate and lactate from lignin. *Metabolic Engineering*, 28, 240–247.  
702 doi:10.1016/j.ymben.2015.01.005  
703
- 704 Kamariotaki, M., Karaliota, A., Stabaki, D., Bakas, T., Perlepes, S. P., & Hadjiliadis, N. (1994).  
705 Coordination complexes of iron(III) with 3-hydroxy-2(1H)-pyridinone, 2,3-  
706 dihydroxybenzoic acid and 3,4-dihydroxybenzoic acid: preparation and characterization  
707 in the solid state. *Transition Metal Chemistry*, 19(2), 241–247. doi:10.1007/BF00161899  
708
- 709 Larsson, S., Palmqvist, E., Hahn-Hägerdal, B., Tengborg, C., Stenberg, K., Zacchi, G., &  
710 Nilvebrant, N.-O. (1999). The generation of fermentation inhibitors during dilute acid  
711 hydrolysis of softwood. *Enzyme and Microbial Technology*, 24(3-4), 151–159.  
712 doi:10.1016/S0141-0229(98)00101-X  
713
- 714 Lennen, R. M., Kruziki, M. A., Kumar, K., Zinkel, R. A., Burnum, K. E., Lipton, M. S., ...  
715 Pfleger, B. F. (2011). Membrane stresses induced by overproduction of free fatty acids in  
716 *Escherichia coli*. *Applied and Environmental Microbiology*, 77(22), 8114–8128.  
717 doi:10.1128/AEM.05421-11  
718
- 719 Linger, J. G., Vardon, D. R., Guarnieri, M. T., Karp, E. M., Hunsinger, G. B., Franden, M. A., ...  
720 Beckham, G. T. (2014). Lignin valorization through integrated biological funneling and  
721 chemical catalysis. *Proceedings of the National Academy of Sciences of the United States*  
722 *of America*, 111(33), 12013–12018. doi:10.1073/pnas.1410657111  
723
- 724 McMahon, B., & Mayhew, S. G. (2007). Identification and properties of an inducible  
725 phenylacetyl-CoA dehydrogenase in *Pseudomonas putida* KT2440. *FEMS Microbiology*  
726 *Letters*, 273(1), 50–57. doi:10.1111/j.1574-6968.2007.00780.x  
727
- 728 Meijnen, J.-P., de Winde, J. H., & Ruijsenaars, H. J. (2008). Engineering *Pseudomonas putida*  
729 S12 for efficient utilization of D-xylose and L-arabinose. *Applied and Environmental*  
730 *Microbiology*, 74(16), 5031–5037. doi:10.1128/AEM.00924-08  
731
- 732 Miyada, C. G., Stoltzfus, L., & Wilcox, G. (1984). Regulation of the *araC* gene of *Escherichia*  
733 *coli*: catabolite repression, autoregulation, and effect on *araBAD* expression. *Proceedings*  
734 *of the National Academy of Sciences of the United States of America*, 81(13), 4120–4124.  
735 doi:10.1073/pnas.81.13.4120  
736
- 737 Müller, J., MacEachran, D., Burd, H., Sathitsuksanoh, N., Bi, C., Yeh, Y.-C., ... Beller, H. R.  
738 (2013). Engineering of *Ralstonia eutropha* H16 for autotrophic and heterotrophic  
739 production of methyl ketones. *Applied and Environmental Microbiology*, 79(14), 4433–  
740 4439. doi:10.1128/AEM.00973-13  
741
- 742 Ouyang, S.-P., Liu, Q., Fang, L., & Chen, G.-Q. (2007). Construction of *pha*-operon-defined  
743 knockout mutants of *Pseudomonas putida* KT2442 and their applications in  
744 poly(hydroxyalkanoate) production. *Macromolecular Bioscience*, 7(2), 227–233.  
745 doi:10.1002/mabi.200600187  
746



- 747 Ouyang, S.-P., Luo, R. C., Chen, S.-S., Liu, Q., Chung, A., Wu, Q., & Chen, G.-Q. (2007).  
748 Production of polyhydroxyalkanoates with high 3-hydroxydodecanoate monomer content  
749 by *fadB* and *fadA* knockout mutant of *Pseudomonas putida* KT2442. *Biomacromolecules*,  
750 8(8), 2504–2511. doi:10.1021/bm0702307  
751
- 752 Pandey, M. P., & Kim, C. S. (2011). Lignin depolymerization and conversion: A review of  
753 thermochemical methods. *Chemical Engineering & Technology*, 34(1), 29–41.  
754 doi:10.1002/ceat.201000270  
755
- 756 Rocha, R. C. S., da Silva, L. F., Taciro, M. K., & Pradella, J. G. C. (2008). Production of poly(3-  
757 hydroxybutyrate-co-3-hydroxyvalerate) P(3HB-co-3HV) with a broad range of 3HV  
758 content at high yields by *Burkholderia sacchari* IPT 189. *World Journal of Microbiology*  
759 & *Biotechnology*, 24(3), 427–431. doi:10.1007/s11274-007-9480-x  
760
- 761 Salvachúa, D., Mohagheghi, A., Smith, H., Bradfield, M. F. A., Nicol, W., Black, B. A., ...  
762 Beckham, G. T. (2016). Succinic acid production on xylose-enriched biorefinery streams  
763 by *Actinobacillus succinogenes* in batch fermentation. *Biotechnology for Biofuels*, 9, 28.  
764 doi:10.1186/s13068-016-0425-1  
765
- 766 Schwalbach, M. S., Keating, D. H., Tremaine, M., Marner, W. D., Zhang, Y., Bothfeld, W., ...  
767 Landick, R. (2012). Complex physiology and compound stress responses during  
768 fermentation of alkali-pretreated corn stover hydrolysate by an *Escherichia coli*  
769 ethanologen. *Applied and Environmental Microbiology*, 78(9), 3442–3457.  
770 doi:10.1128/AEM.07329-11  
771
- 772 Vardon, D. R., Franden, M. A., Johnson, C. W., Karp, E. M., Guarnieri, M. T., Linger, J. G., ...  
773 Beckham, G. T. (2015). Adipic acid production from lignin. *Energy & Environmental*  
774 *Science*, 8(2), 617–628. doi:10.1039/C4EE03230F  
775
- 776 Vizcaíno, J. A., Csordas, A., del-Toro, N., Dianas, J. A., Griss, J., Lavidas, I., ... Hermjakob, H.  
777 (2016). 2016 update of the PRIDE database and its related tools. *Nucleic Acids Research*,  
778 44(D1), D447–56. doi:10.1093/nar/gkv1145  
779
- 780 Wu, W., Dutta, T., Varman, A. M., Eudes, A., Manalansan, B., Loqué, D., & Singh, S. (2017).  
781 Lignin Valorization: Two hybrid biochemical routes for the conversion of polymeric  
782 lignin into value-added chemicals. *Scientific Reports*, 7(1), 8420. doi:10.1038/s41598-  
783 017-07895-1  
784
- 785 You, S. Y., Cosloy, S., & Schulz, H. (1989). Evidence for the essential function of 2,4-dienoyl-  
786 coenzyme A reductase in the beta-oxidation of unsaturated fatty acids in vivo. Isolation  
787 and characterization of an *Escherichia coli* mutant with a defective 2,4-dienoyl-coenzyme  
788 A reductase. *The Journal of Biological Chemistry*, 264(28), 16489–16495.  
789
- 790 Zakzeski, J., Bruijninx, P. C. A., Jongerius, A. L., & Weckhuysen, B. M. (2010). The catalytic  
791 valorization of lignin for the production of renewable chemicals. *Chemical Reviews*,  
792 110(6), 3552–3599. doi:10.1021/cr900354u

793 Zhang, F., Carothers, J. M., & Keasling, J. D. (2012). Design of a dynamic sensor-regulator  
794 system for production of chemicals and fuels derived from fatty acids. *Nature*  
795 *Biotechnology*, 30(4), 354–359. doi:10.1038/nbt.2149  
796  
797

798 **TABLES**

799

800 **Table 1.** Bacterial strains and plasmids used in this study.

Strain or plasmid	Relevant genotype or description	Source or reference	JBEI ID
<i>P. putida</i>			
mt-2		ATCC 33015	JPUB_011085
JD1	mt-2 with deletion of <i>pha</i> operon	This study	JPUB_011086
JD2	mt-2 with deletion of <i>fadAB</i>	This study	JPUB_011087
JD3	mt-2 with deletion of both <i>pha</i> operon and <i>fadAB</i>	This study	JPUB_011088
JD4	mt-2 with deletion of both <i>pha</i> operon and <i>fadAB</i> , containing pJM2	This study	JPUB_011089
JD5	mt-2 with deletion of <i>fadAB</i> operon, containing pJM20	This study	-
JD6	mt-2 with deletion of <i>pha</i> operon, containing pJM20	This study	-
<i>E. coli</i>			
S17-1	<i>recA pro hsdR</i> RP4-2-Tc::Mu-Km::Tn7 integrated into the chromosome	ATCC 47055	JPUB_011083
DH5 $\alpha$		Thermo Fisher Scientific	-
JD7	S17-1 containing pJD1	This study	JPUB_011093
JD8	S17-1 containing pJD2	This study	JPUB_011094
EGS1895	DH1; $\Delta$ <i>fadE</i> ; $\Delta$ <i>fadA</i> ; $\Delta$ <i>ackA-pta</i> ; $\Delta$ <i>poxB</i> , with <i>fadR</i> , <i>fadD</i> , <i>fadM</i> , ' <i>tesA</i> , <i>fadB</i> , <i>co_aco</i>	Goh et al., 2014	JPUB_011082
Plasmids			
pK18mobsacB	suicide plasmid for gene knockout, Kam <sup>R</sup>	ATCC	JPUB_011084
pJD1	pK18mobsacB containing partial deleted <i>pha</i> operon	This study	JPUB_011092
pJD2	pK18mobsacB containing partial deleted <i>fadAB</i> gene	This study	JPUB_011094
pJM20	pBBR1-MCS2 containing ' <i>tesA</i> , <i>fadB</i> , <i>Mlut_11700</i> , and <i>fadM</i> under the control of P <sub>BAD</sub> (2-bp deletion in 3'-end).	Müller et al., 2013	JPUB_011090

801 “-“ indicates the strain was not archived

802

803

804 **Table 2.** Measured components in biomass hydrolysates.

	<i>A. thaliana</i> WT (g/L) <sup>a</sup>	<i>A. thaliana</i> QsuB (g/L)	<i>A. thaliana</i> HCHL (g/L)	Switchgrass (g/L)
Glucose	1.94±0.05	2.91±0.01	2.61±0.02	5.02±0.10
Xylose	2.05±0.05	2.41±0.00	2.18±0.01	4.19±0.10
Arabinose	-	-	0.044±0.000	0.59±0.03
Amino acids <sup>b</sup>	0.25±0.07	0.33±0.00	0.85±0.08	1.16±0.07
PCA	-	1.04±0.02	-	-
4-HB	-	-	0.20±0.00	0.006±0.001
<i>p</i> -Coumarate	-	-	-	0.074±0.002
Ferulate	-	-	-	0.063±0.002
Acetate	0.49±0.01	0.54±0.00	0.53±0.01	0.73±0.01

805 <sup>a</sup> This *A. thaliana* WT is the wild-type control of the HCHL line.

806 <sup>b</sup> This is the total concentration of amino acids. See Figure 4A for more detailed profiles.

807 “-” indicates the concentration is <0.001 g/L.

808 **FIGURES**

809

810 **Figure 1.** Methyl ketone production from *P. putida* strain JD4. *P. putida* JD4 was grown with  
811 2% glucose (Glu), 1.5% *p*-hydroxybenzoate (4-HB) and 1% protocatechuate (PCA). Decane (2  
812 mL) was overlaid onto the cultures when arabinose (0.2%) was added at 6 h to induce methyl  
813 ketone production. Titers are reported for methyl ketones in decane overlay at 48 h. Cultures  
814 were performed in triplicate and error reported as  $\pm$  standard deviation.

815

816 **Figure 2.** A) HPLC measurements of glucose (Glu), xylose (Xyl) and monoaromatics (4-HBA,  
817 PCA) released from *A. thaliana* biomass by sequential dilute acid and enzymatic hydrolysis. *A.*  
818 *thaliana* QsuB and HCHL lines were compared to their respective wild type (WT) controls.  
819 Measurements were performed in triplicate and error reported as  $\pm$  standard deviation; B) Methyl  
820 ketone production by *P. putida* JD4 with hydrolysates derived from *A. thaliana* biomass.  
821 Cultures with *A. thaliana* hydrolysates were compared to a control containing 3 g/L of glucose  
822 and 2 g/L of xylose (Glu/Xyl). Methyl ketone production was performed as described in the  
823 Figure 1 legend; C) *E. coli* EGS1895 methyl ketone production with the same *A. thaliana*  
824 hydrolysates and Glu/Xyl control as the experiment with *P. putida* JD4.

825

826 **Figure 3.** A) HPLC measurements of glucose (Glu) and xylose (Xyl) released by sequential and  
827 separate dilute acid and enzymatic hydrolysis of switchgrass. Measurements were performed in  
828 triplicate and error reported as  $\pm$  standard deviation; B) Methyl ketone production by *P. putida*  
829 JD4 with switchgrass hydrolysates. Cultures with switchgrass hydrolysates were compared to a  
830 control containing 5 g/L of glucose and 4 g/L of xylose (Glu/Xyl). Methyl ketone production at  
831 48 h was performed as described in the Figure 1 legend; C) *E. coli* EGS1895 methyl ketone  
832 production at 72 h with the same switchgrass hydrolysates and Glu/Xyl control as the experiment  
833 with *P. putida* JD4.

834

835 **Figure 4.** Comparative proteomics of fatty acid metabolism of *P. putida* JD4 during methyl  
836 ketone production. Normalized spectral counts of selected proteins (Table S1) were compared  
837 for *P. putida* JD4 cultures grown for 24 h with glucose/xylose as carbon sources, or with  
838 hydrolysates from *A. thaliana* HCHL and switchgrass biomass. The graph depicts the fold  
839 change observed between the cultures grown on hydrolysate and sugar-only control.

840

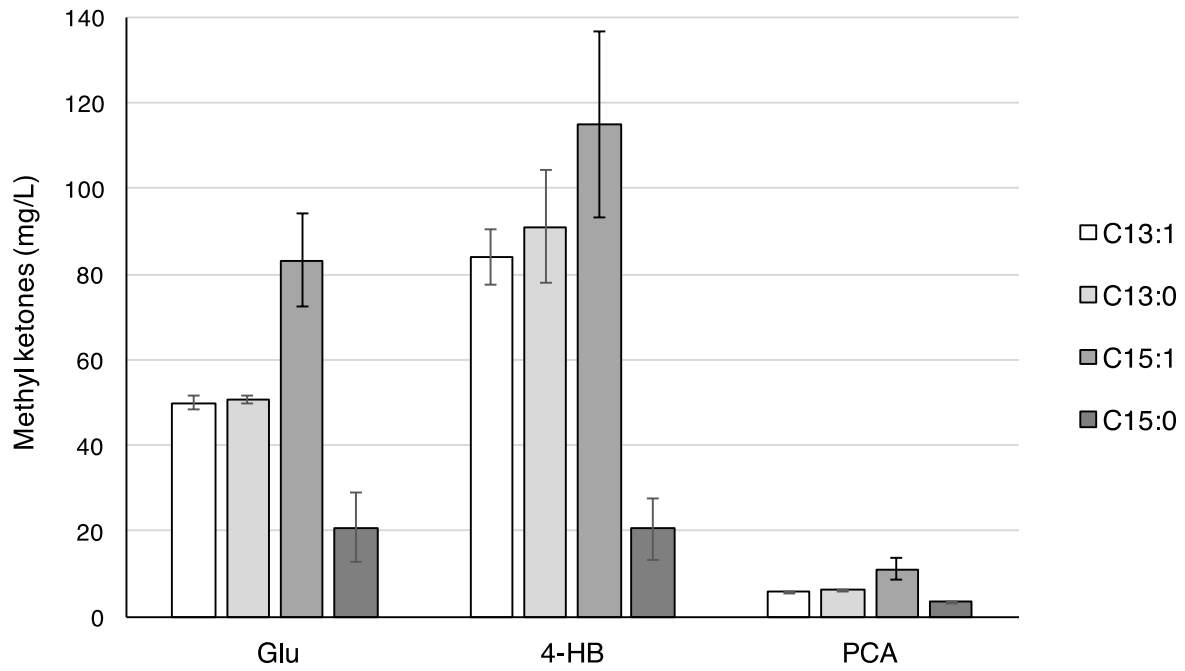
841 **Figure 5.** A) LC-MS measurements of amino acid concentrations in acid hydrolysates obtained  
842 by pretreatment of *A. thaliana* HCHL line, switchgrass and sorghum. B) Correlation of amino  
843 acid concentration in hydrolysates and methyl ketone production by *P. putida* JD4. Methyl  
844 ketone production was performed as described in the Figure 1 legend.

845

846 **Figure 6.** Methyl ketone production in minimal medium supplemented with amino acids. *P.*  
847 *putida* JD4 was cultured on minimal medium with 5 g/L of glucose as the substrate (Glu). The  
848 medium was amended with a defined mixture of amino acids (Ser, Val, Asp, Phe and Trp) at  
849 total concentrations from 0.5-1.5 g/L. Methyl ketone production at 48 h was performed as  
850 described in the Figure 1 legend.

851

852 **Figure 1**  
853

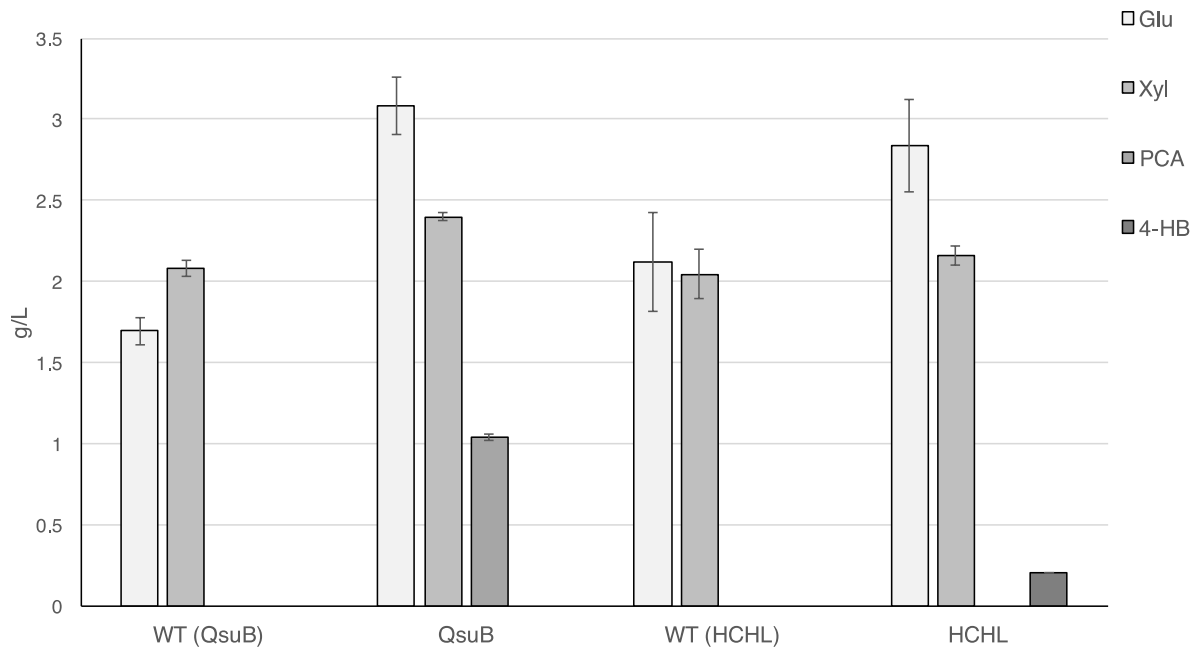


854  
855  
856

857 **Figure 2**

858

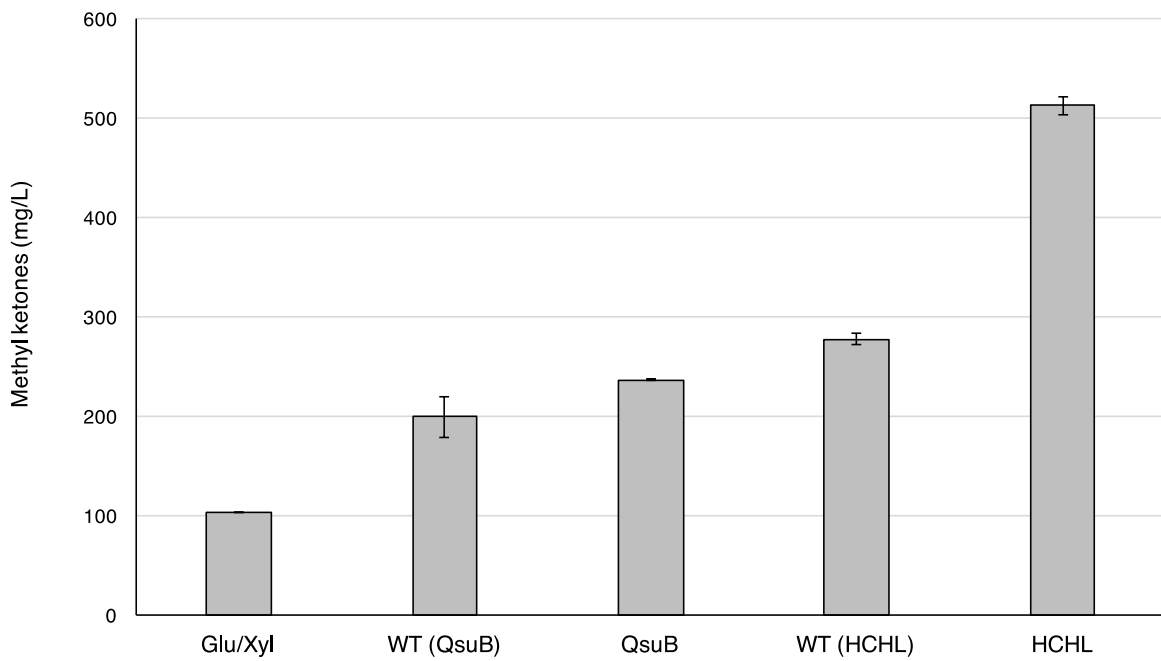
859 **A**



860

861 **B**

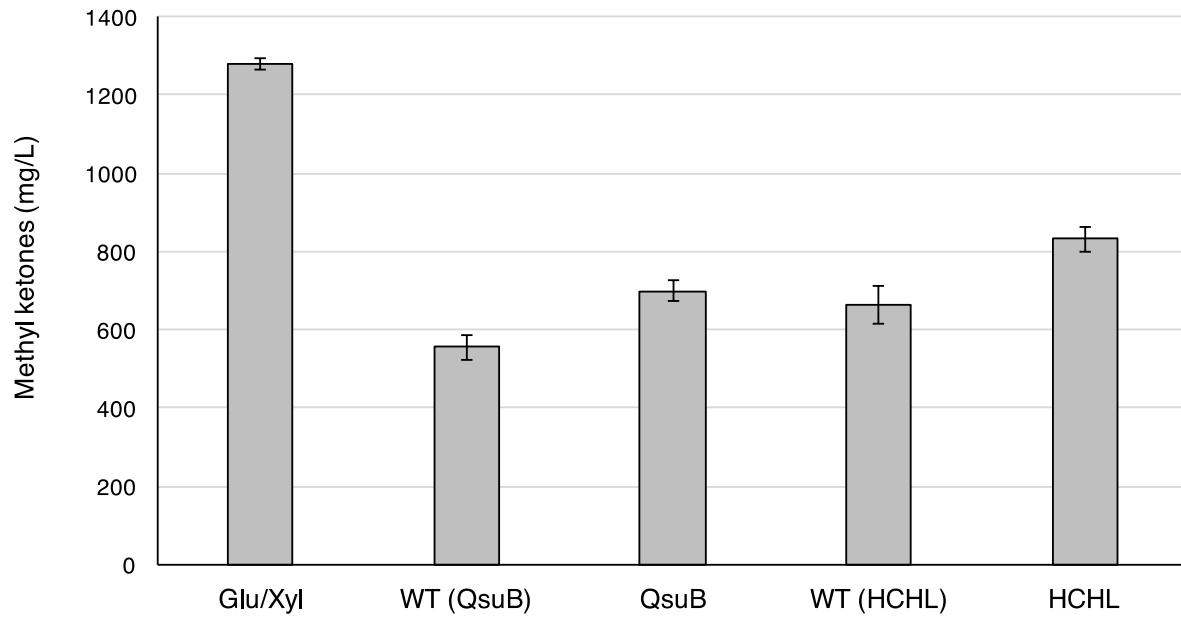
862



863

864

865 **C**  
866



867  
868  
869

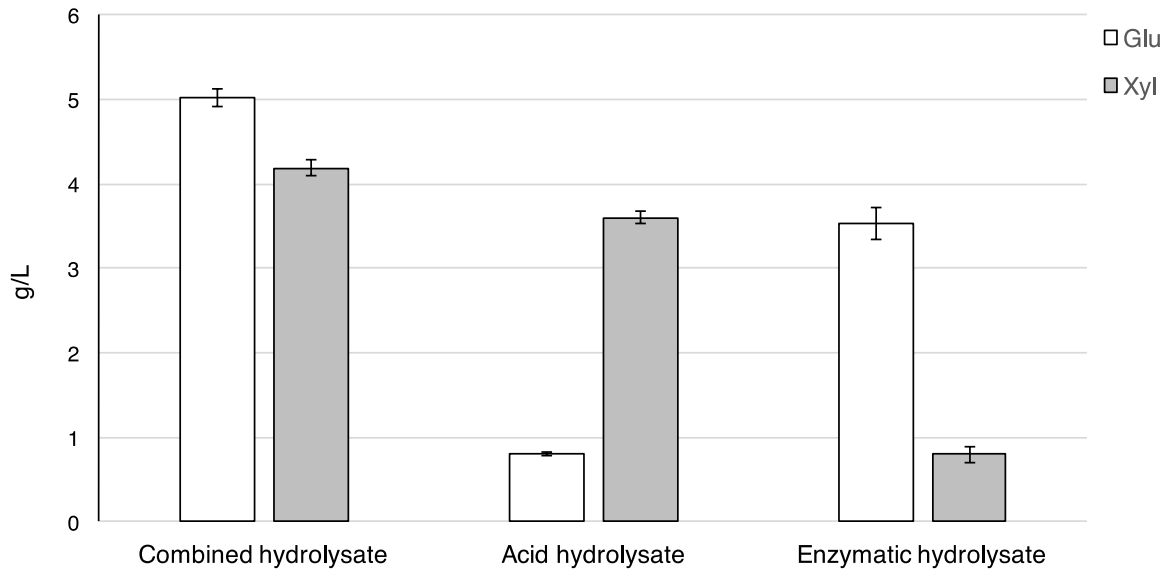


870 **Figure 3**

871

872 **A**

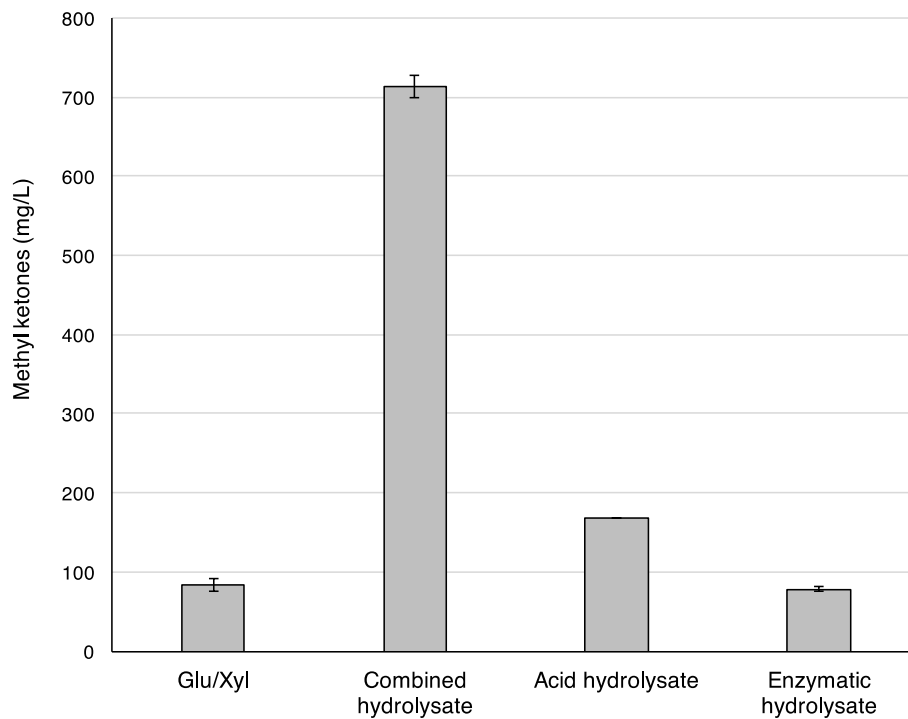
873



874

875 **B**

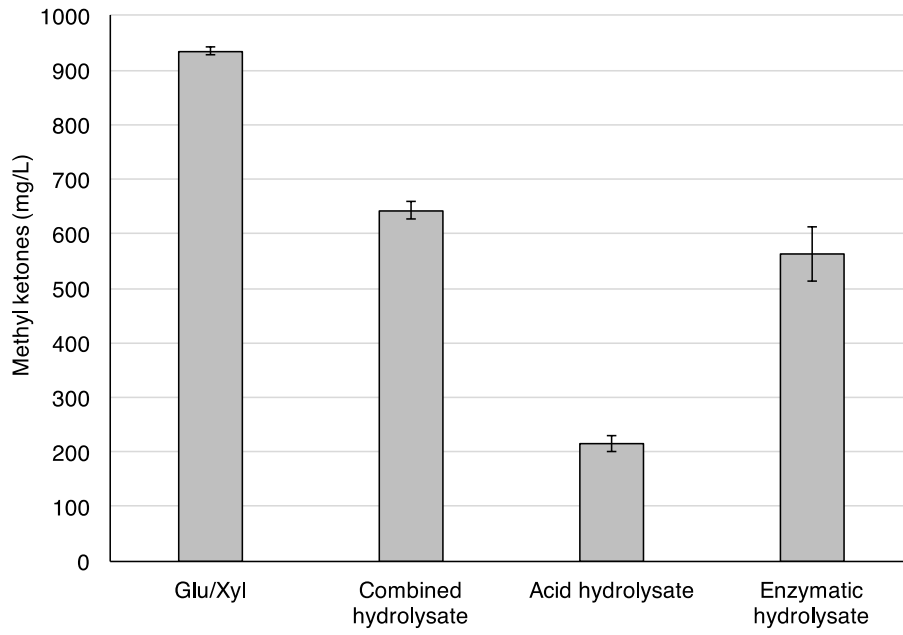
876



877

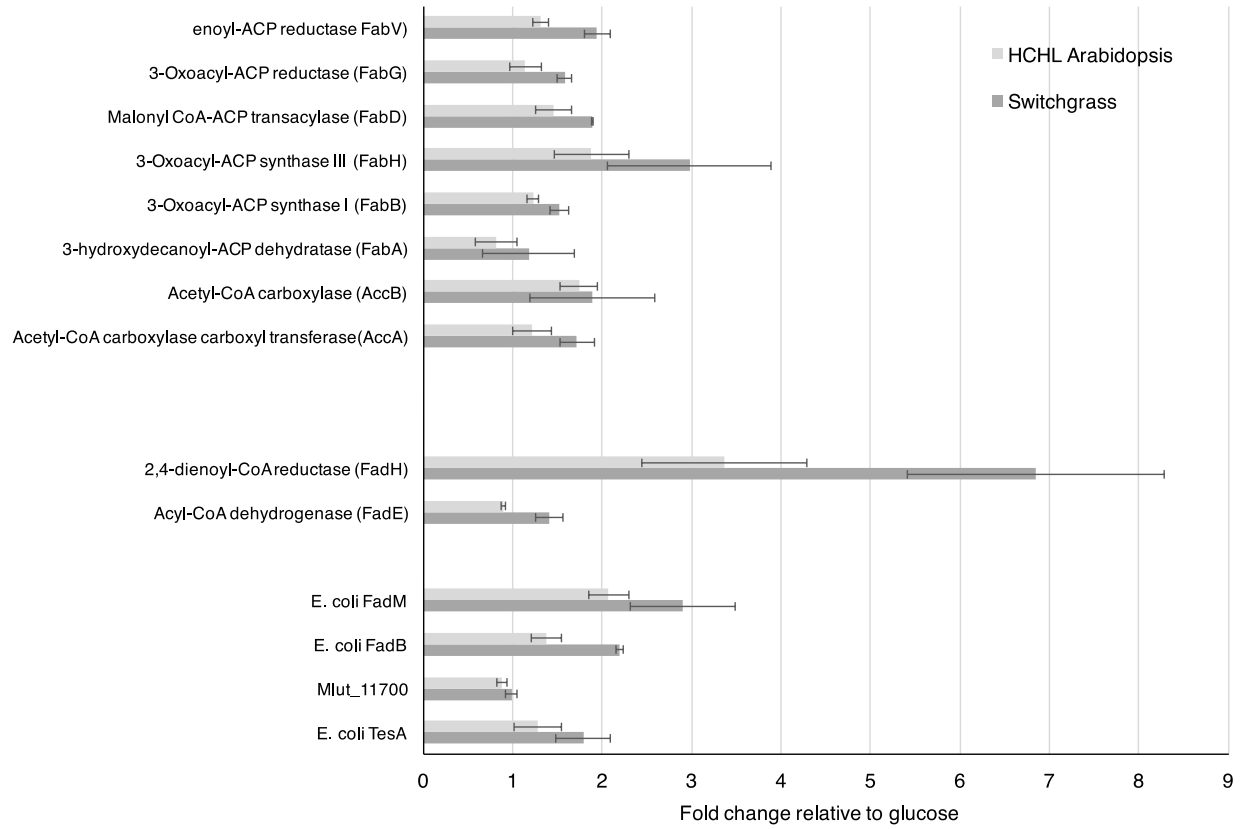
878

879 **C**  
880



881  
882

883 **Figure 4**  
884



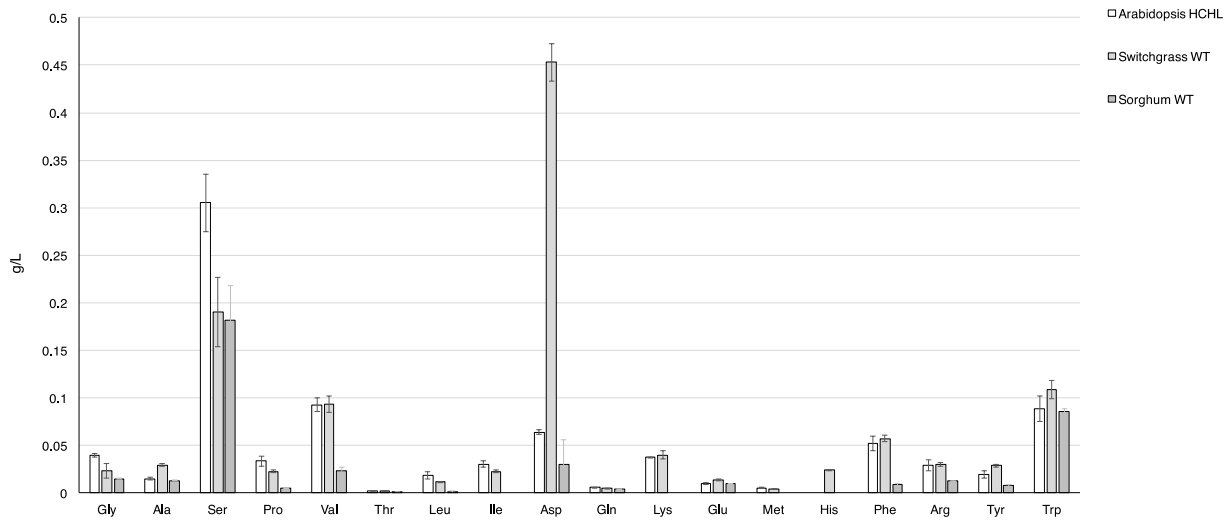
885  
886

887 **Figure 5**

888

889 **A**

890

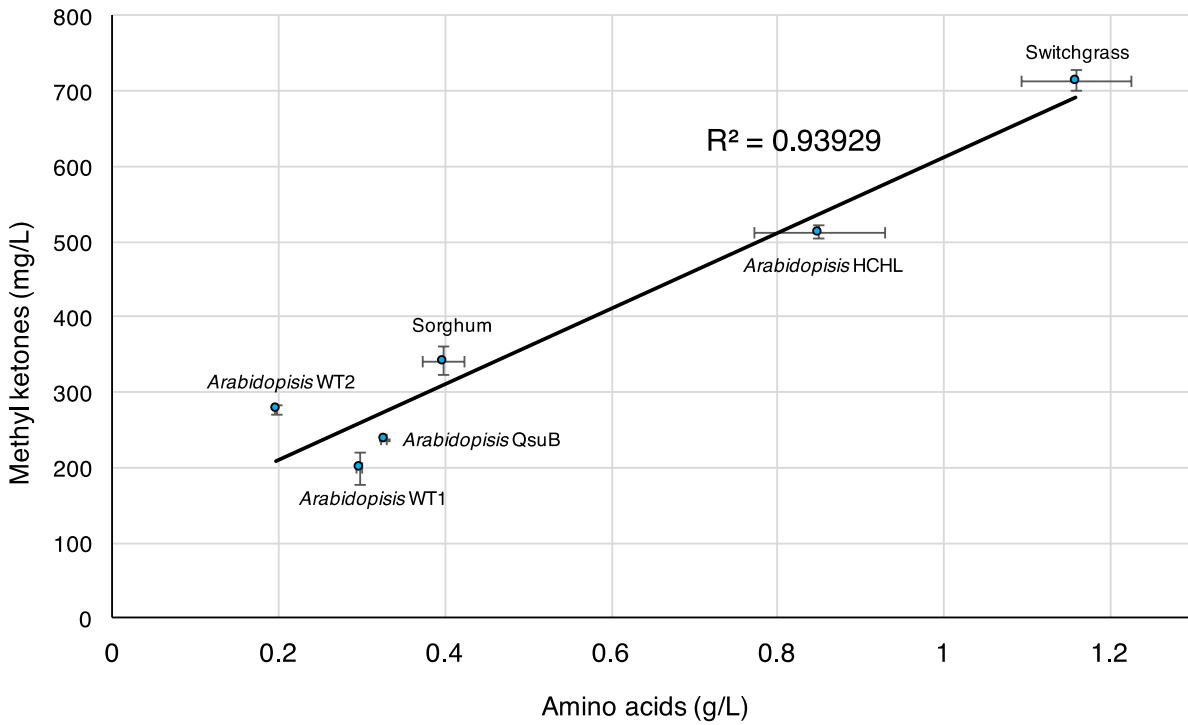


891

892

893 **B**

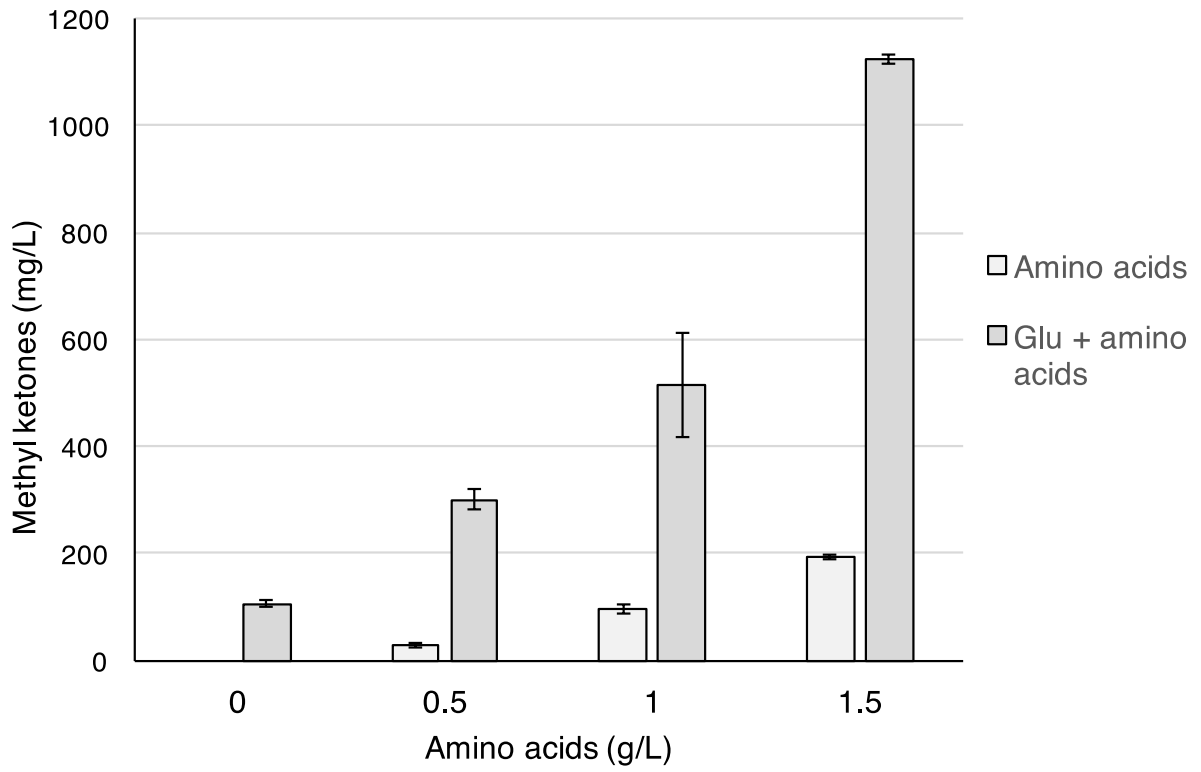
894



895

896

897 **Figure 6**  
898



899